ACS APPLIED MATERIALS & INTERFACES

Research Article

www.acsami.org

Immobilization of Carbon Dots in Molecularly Imprinted Microgels for Optical Sensing of Glucose at Physiological pH

Hui Wang, Jinhui Yi, David Velado, Yanyan Yu, and Shuiqin Zhou*

Department of Chemistry of The College of Staten Island, The City University of New York, Staten Island, 10314 New York, United States

Ph.D. Program in Chemistry, The Graduate Center of the City University of New York, New York, 10016 New York, United States

Supporting Information

ABSTRACT: Nanosized carbon dots (CDs) are emerging as superior fluorophores for biosensing and a bioimaging agent with excellent photostability, chemical inertness, and marginal cytotoxicity. This paper reports a facile one-pot strategy to immobilize the biocompatible and fluorescent CDs (~6 nm) into the glucose-imprinted poly(*N*-isopropylacrylamide-acrylamide-vinylphenylboronic acid) [poly(NIPAM-AAm-VPBA)] copolymer microgels for continuous optical glucose detection. The CDs designed with surface hydroxyl/carboxyl groups can form complexes with the AAm comonomers via hydrogen bonds and, thus, can be easily immobilized into the gel network during the polymerization reaction. The resultant glucose-imprinted hybrid microgels can reversibly swell and shrink in response to the variation of surrounding glucose concentration and correspondingly quench and recover the fluorescence signals of the embedded CDs, converting biochemical signals to optical signals. The highly imprinted hybrid microgels demonstrate much higher sensitivity and selectivity for glucose detection than the nonimprinted hybrid microgels over a clinically relevant range of 0−30 mM at physiological pH and benefited from the synergistic effects of the glucose molecular contour and the geometrical constraint of the binding sites dictated by the glucose imprinting process. The highly stable immobilization of CDs in the gel networks provides the hybrid microgels with excellent optical signal reproducibility after five repeated cycles of addition and dialysis removal of glucose in the bathing medium. In addition, the hybrid microgels show no effect on the cell viability in the tested concentration range of 25−100 μg/mL. The glucose-imprinted poly(NIPAM-AAm-VPBA)-CDs hybrid microgels demonstrate a great promise for a new glucose sensor that can continuously monitor glucose level change.

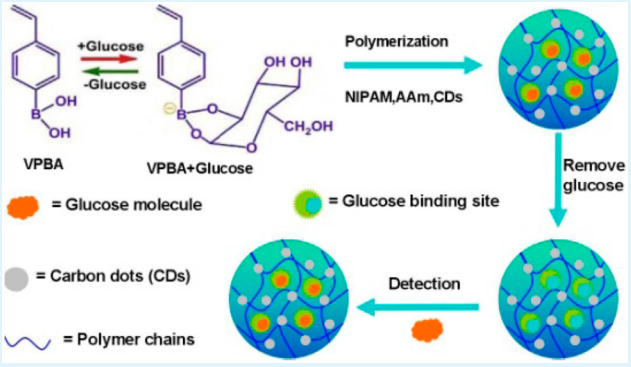

KEYWORDS: *carbon dots, molecular imprinting, hybrid microgels, glucose sensing, physiological pH*

1. INTRODUCTION

The detection of glucose concentration in the body fluid has attracted continuous attention for several decades because it is a fundamental part in the management of diabetes mellius, a complex metabolism disease with a rapid increase in patient populations.[1] Currently, nearly all commercially available glucose sensors function by indirect electrochemical detection of hydrogen peroxide produced by enzymatic oxidation of glucose with glucose oxidase. The enzyme-based approach is straightforward to measure the glucose level in the collected blood sample, but it faces many more challenges for continuous monitoring due to the limitations of instability, difficult sterilization, slow sensor time lags, and high cost.[2,3] Furthermore, collection of blood samples for glucose testing often involves frequent, inconvenient, and potentially painful finger pricks, making patients reluctant to test regularly. In contrast, fluorescence detection of glucose based on the reversible binding with specific ligands will not only provide high sensitivity, selectivity, and reproducibility but also have great potential to realize continuous and noninvasive (or minorly invasive) diabetes control. Consequently, there is widespread research interest in the development of optical continuous glucose sensors based on reversible glucose binding with boronic acids,[4,5] including the polymerized crystalline colloidal array,[6,7] holographic thin films,[8] glucose-mediated assembly of fluorescent dyes and quantum dots (QDs),[9−11] and hybrid nanogels embedded with dyes and inorganic nanoparticles.[12−17] In particular, the hybrid nanogel-based glucose sensors developed by us have several favorable advantages, including rapid response time, easy engineering on surface, potential biocompatibility, and porous structures for loading insulin and simultaneous glucose-regulated insulin delivery.[16,17] In addition, they can be potentially fabricated into hydrogel-based soft contact lens sensors for glucose detection, which is

Received: February 23, 2015
Accepted: July 6, 2015
Published: July 6, 2015

DOI: 10.1021/acsami.5b04744
ACS Appl. Mater. Interfaces 2015, 7, 15735−15745

portable and disposable with no need of electrodes or electric circuits. So far, a variety of optical markers have been explored to prepare the boronic acid based hybrid nanogels for continuous glucose sensors, including fluorescent organic dyes, semiconductor QDs, and noble metal nanoparticles (NPs).[12−20] However, these optical markers have potential problems for practical applications. For example, organic dyes are concerned with poor photostability and potential toxicity, semiconductor QDs are associated with the inherent heavy metal toxicity, and noble metal materials involve high cost. Sun's group have developed a series of new NPs for optical detection of glucose, including carbon nitride dots,[21] Fe(III)-based coordination polymer NPs,[22] polyoxometalate clusters,[23] CoFe layered double hydroxide nanopalates,[24] mesoporous Fe_2O_3-graphene nanosheet and graphitic carbon nitride nanosheets.[25,26] While these optical sensors demonstrate rapid and highly sensitive detection ability for glucose, they are not suitable for continuous glucose sensing because the method is still based on the indirect detection of hydrogen peroxide produced by enzymatic oxidation of glucose with glucose oxidase.

Recently, carbon dots (CDs) have gained tremendous attention for their unique and tunable photoluminescence (PL) properties.[27−36] CDs are a group of three-dimensional carbon nanomaterials with sp^2 character, a symbolic of nanocrystalline graphite. These CDs can readily exhibit quantum effects when their size is below 10 nm. The recent research results indicate that CDs combine a number of key merits, including excellent photostability, small size, biocompatibility, highly tunable PL property, up-conversion PL property, electrochemiluminescence, and chemical inertness and, thus, are continuously being explored as an alternative for dye-based probes and toxic QDs in many biological applications.[28−36] While CDs emerge as superior and universal fluorophores, very limited studies were carried out to use the CDs as optical probe for glucose sensing. Very recently, Xia et al. synthesized boronic acid functionalized CDs based on the one-step hydrothermal decomposition of phenylboronic acids. The glucose mediated assembly of these CDs demonstrated an ultrahigh sensitivity for glucose detection with a linear range of 9−900 μM and a detection limit as low as 1.5 μM.[37] While these CDs are highly sensitive and useful for glucose detection at low concentration range, there are number of disadvantages of this type of glucose sensor. First, the detectable linear range of the glucose level below 0.90 mM is not in the typical clinically relevant blood glucose concentration range for diabetic patients. Second, it takes about an hour for the glucose-mediated assembly of the CDs to reach the stable optical signal reading. The slow assembling/disassembling process of these CDs is also not suitable for continuous glucose monitoring.

Herein, we report a facile one-pot strategy to immobilize the biocompatible and fluorescent CDs into the glucose imprinted polymer microgel network for highly sensitive and selective glucose detection at physiological pH. As shown in Figure 1, three functional comonomers [*N*-isopropylacyamide (NIPAM), acrylamide (AAm), and 4-vinylphenyl boronic acid (VPBA)] and fluorescent CDs placed in one pot can be readily fabricated into monodispersed CDs-embedded hybrid microgels via a free radical precipitation polymerization in water. Specifically, NIPAM was designed to enable the precipitation polymerization of these water-soluble comonomers at the reaction temperature (70 °C) above the lower critical solution temperature of the resultant polyNIPAM-dominant copolymers. AAm was designed to (1) complex with the fluorescent CDs through hydrogen bonding interactions between the amide group of AAm and the surface hydroxyl/carboxyl groups on CDs, and (2) improve the glucose sensitivity of the microgels at physiological pH through the weak Lewis acid−base interactions between the electron-poor boron atom in VPBA units and the electron-rich nitrogen atom in the adjacent AAm units.[16] VPBA with a boronic acid moiety was designed for reversible glucose binding, which is pH-dependent. At the rationally designed pH value (pH 8.8) of the reaction medium, the glucose molecules and the VPBA monomers form stable negatively charged glucose−VPBA complex. After the copolymerization and cross-linking of the NIPAM, AAm−CDs complexes, and glucose−VPBA complexes, the CDs remain binding with AAm units and the glucose molecules remain binding on the PBA moieties in the resulted poly(NIPAM-AAm-VPBA) copolymer networks. Such synthesized hybrid microgels will have small CDs randomly immobilized in the gel network. On the other hand, the glucose-PBA binding is not favorable in neutral water. Thus, the glucose molecules originally binding on the PBA moieties can be freed and diffuse out from the gel network when the microgels are dispersed into deionized water. After dialysis removal of these glucose molecules, the glucose-imprinted boron centers will serve as favorable glucose recognition sites and thus provide high selectivity and sensitivity for glucose detection. We expect that such glucose-imprinted poly(NIPAM-AAm-VPBA)-CDs hybrid microgels will undergo a volume phase transition in response to the variation of glucose concentrations in the dispersion medium, which could change the physicochemical environment of the fluorescent CDs stably immobilized in the gel network and, hence, convert the biochemical signals into fluorescent signals with excellent reproducibility. Such designed glucose-imprinted poly(NIPAM-AAm-VPBA)-CDs hybrid microgels will combine several key merits into a single glucose sensor, including simple preparation, good biocompatibility of hydrogels and CDs, excellent structural stability and chemical inertness, stable and tunable fluorescent properties, and highly sensitive, selective, and reversible binding with glucose

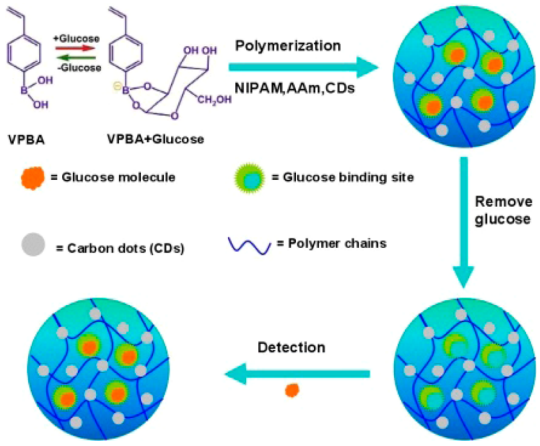

Figure 1. Schematic synthetic illustration of the glucose-imprinted poly(NIPAM-AAm-VPBA)-CDs hybrid microgels with specific glucose-binding sites for highly sensitive and selective glucose detection, based on the one-step free radical precipitation polymerization in water. The CDs are randomly immobilized in the imprinted poly(NIPAM-AAm-VPBA) microgel networks through hydrogen bonding interactions between the amide groups of AAm and the surface hydroxyl/carboxyl groups on CDs.

DOI: 10.1021/acsami.5b04744
ACS Appl. Mater. Interfaces 2015, 7, 15735−15745

molecules. Furthermore, such fluorescence-based hybrid microgels can be easily fabricated into miniature glucose sensor device with no need of electrodes or electric circuits (e.g., portable and disposable soft hydrogel-based contact lens), thus have great potential to realize continuous and noninvasive diabetes control.

2. EXPERIMENTAL METHODS

2.1. Materials. D(t)-Glucose was purchased from ACROS, and all other chemicals were purchased from Aldrich. NIPAM was recrystallized from a 1:1 hexane−acetone mixture and dried in vacuum. 4-Vinylphenylboronic acid (VPBA), acrylamide (AAm), *N*,*N*′-methylenebis(acrylamide) (BIS), 2,2′-azobis(2-methylpropionamidine) dihydrochloride (AAPH), sodium dodecyl sulfate (SDS), sodium hydroxide (NaOH), HCl (37%), sodium L-lactate, and human serum albumin (HSA) were used as received without further purification. The water used in all experiments was of Millipore Milli-Q grade.

2.2. Synthesis of Fluorescent Carbon Dots (CDs). In a typical synthesis, glucose (2.70 g) was dissolved in deionized water (10 mL). After intense sonication for 20 min, 30.0 mL of HCl (37 wt %) was slowly added into the above solution. The mixed solution was then treated ultrasonically for 8 h and transferred into a 50 mL Teflon-lined stainless autoclave. The precursor solution was heated to and maintained at 200 °C. After 24 h, the solution was cooled naturally to room temperature. The resulted CDs were purified with repeated centrifugation and redispersion in water for three cycles. Finally, the aqueous dispersion of CDs was dialyzed for 7 days (Spectra/Por molecular porous membrane tubing, cutoff 12,000−14,000) at room temperature (~22 °C). The aqueous dispersion of CDs was then collected and dried to get solid CDs.

2.3. Synthesis of Glucose-Imprinted Poly(NIPAM-AAm-VPBA)-CDs Hybrid Microgels. In a 250 mL round-bottom flask equipped with a stirrer, a N_2 gas inlet, and a condenser, 97 mL aqueous suspension of CDs (0.1 mg/mL, pH 8.8) was first added, followed with the addition of suitable amount of glucose (0, 0.147, and 0.295 g) and VPBA (0.242 g). The mixture solution was heated to 70 °C for 30 min and then NIPAM (0.7024 g), AAm (0.059 g), BIS (0.0368 g), and SDS (0.0254 g) were added into this mixture solution under stirring. After a continuous N_2 purge for 60 min at 70 °C, the polymerization was initiated by adding 3.00 mL of a AAPH solution of 0.105 M. The polymerization reaction was allowed to proceed for 5 h. The solution was centrifuged three times at 20,000 rpm (30 min, Thermo Electron Co. SORVALLRC-6 PLUS superspeed centrifuge) with the supernatant discarded and the precipitate redispersed in 100 mL of very dilute NaOH aqueous solution of pH 8.8. To remove the imprinting glucose molecules, possible unreacted monomers, and free CDs, the resultant hybrid microgels with a volume of 100 mL were further purified by 10 days of dialysis (Spectra/Por molecular porous membrane tubing, cutoff 12000−14000, Dalton MWCO) against very frequently changed water at room temperature. The resulting glucose-imprinted hybrid microgels were coded as IHM-0, IHM-147, and IHM-295, respectively, corresponding to different imprinting degree with 0, 0.147, and 0.295 g of glucose used for imprinting purpose in the synthesis. In addition, glucose (0.295 g)-imprinted poly(NIPAM-AAm-VPBA) microgels (coded as IM-295) without the presence of CDs was prepared for a control comparison.

2.4. In Vitro Cytotoxicity of CDs, Nonimprinted Hybrid Microgels, and Imprinted Hybrid Microgels. B16F10 cells were cultured in the 96 wells microplate in 100 μL of medium containing about 2000 cells seeded into each wells. After an overnight incubation for attachment, the medium was removed and another 100 μL of medium containing CDs, nonimprinted hybrid microgels or imprinted hybrid microgels was added to make the final exact concentration of 100, 75, 50, and 25 μg/mL, respectively. Wells used the normal medium without any CDs or microgel samples were used as control. After incubated for 24 h, 10 μL of 3-(4,5-dimethyl-2-thiazolyl)-2,5-diphenyltetrazolium bromide (MTT) solution (5 mg/mL in PBS) was added into the wells. The wells were further incubated in a humidified environment of 5% CO_2 and 37 °C for 2 h. The medium was removed after 2 h, and 100 μL of dimethyl sulfoxide was added. The plates were gently agitated until the formazan precipitate was dissolved, followed by measurement of optical density value by spectrophotometer at 570 and 690 nm, respectively.

2.5. Characterization. The UV−vis absorption spectra were obtained on a Thermo Electron Co. Helios β UV−vis spectrometer. The FT-IR spectra were recorded with a Nicolet Instrument Co. MAGNA-IR 750 Fourier transform infrared spectrometer. X-ray electron spectroscopy (XPS) was performed on an ESCALAB 250 X-ray photoelectron spectrometer with Al Kα radiation. The PL spectra were obtained on a JOBIN YVON Co. FluoroMax-3 Spectrofluorometer equipped with a Hamamatsu R928P photomultiplier tube, calibrated photodiode for excitation reference correction from 200 to 980 nm, and an integration time of 1 s. The transmission electron microscopy (TEM) images were taken on a FEI TECNAI transmission electron microscope at an accelerating voltage of 100 kV. High-resolution TEM image was characterized by a JEM 2100 instrument with an acceleration voltage of 200 kV. Dynamic light scattering (DLS) was performed on a standard laser light scattering spectrometer (BI-200SM) equipped with a BI-9000 AT digital time correlator (Brookhaven Instruments Corporation) to measure the hydrodynamic radius (R_h) distributions. A Nd:YAG laser (150 mW, 532 nm) was used as the light source. The hybrid microgel dispersion was passed through Millipore Millex-HV filters with a pore size of 0.80 μm to remove dust before the DLS measurements. The confocal laser scanning microscope (CLSM) images were acquired using a laser scanning microscope Leica SP8X (Leica Microsystems GmbH, Germany).

3. RESULTS AND DISCUSSION

3.1. Synthesis, Composition, and Morphology of the Glucose-Imprinted Hybrid Microgels. Our strategy to prepare the glucose-imprinted hybrid microgels involves the first synthesis of water-dispersible CDs bearing surface carboxyl/hydroxyl groups, followed by one-step free radical precipitation copolymerization of the VPBA (18.54%), NIPAM (70.6%), AAm (8.14%) and CDs in the presence of glucose and BIS (2.72%) at 70 °C and pH 8.8. The purpose to set the pH of the reaction solution at 8.8 is to ensure the stable binding of glucose molecules to the VPBA monomers prior to the copolymerization of all the functional monomers. The PBA groups in aqueous solution are in equilibrium between the undissociated (uncharged) and the dissociated (charged) forms with a pK_a about 8.2. Both forms react reversibly with glucose. However, the complexation of the uncharged PBA with glucose is unstable because it is highly susceptible to hydrolysis, but the binding with glucose causes the thermodynamically more favorable charged form. When pH is well below the pK_a (e.g., pH < 7), the uncharged VPBA monomers will not stably complex with glucose molecules, thus the microgels polymerized from the NIPAM, AAm and free VPBA will not be successfully imprinted by glucose molecules. At a pH value (e.g., pH ~ 8.8) well above the pK_a, nearly all the PBA groups are transferred to the charged form and form stable complex with glucose molecules. However, further increase in pH values of the reaction solution is unnecessary because purification of the microgel product will require a longer dialysis time to remove the hydroxide ions at a higher pH. After the copolymerization of these glucose-complexed VPBA monomers with NIPAM and CDs-complexed AAm comonomers, it is expected that the collective weak interactions between the VPBA monomers and the glucose molecules can form populations of complementary binding sites in the resulted polymer chain networks.[38,39] Specifically, 0, 0.147, and 0.295 g of glucose were respectively used for synthesis of the glucose-

DOI: 10.1021/acsami.5b04744
ACS Appl. Mater. Interfaces 2015, 7, 15735−15745

imprinted hybrid microgels to compare how the glucose-imprinting degree can affect the sensitivity and selectivity of the hybrid microgels for glucose detection. The resulting samples were correspondingly coded as IHM-0, IHM-147, and IHM-295, respectively. The fluorescent CDs used for the synthesis of the imprinted poly(NIPAM-AAm-VPBA)-CDs hybrid microgels were prepared via one-pot acid assisted hydrothermal decomposition of glucose.[40] The typical TEM image of the as-synthesized CDs shows dispersed particles in a spherical shape with an average size of 6.3 nm in diameter (see the Supporting Information Figure S1a). A highly crystalline structure is visible in the high resolution TEM image of the CDs (Figure S1b). The sharp diffraction spots in the typical selected area electron diffraction (SAED) pattern of a single CD (inset in Figure S1b) further indicate the presence of single-crystalline structure of CDs. The size distribution of the CDs (Figure S1c) produces a standard deviation from the mean diameter of 6.33 ± 0.68 nm. The XPS spectrum shown in Figure S 1d clearly reveals that carbon and oxygen are present on the surface of the as-synthesized CDs. As shown in Figure S1e, the CDs display excitation wavelength-dependent PL property. With the increase in the excitation wavelength from 240 to 540 nm, the emission bands red-shifted with the maximum PL intensity located at 512 nm obtained with an excitation wavelength of 440 nm. The PL quantum yield of the CDs was determined to be 9.06% by using rhodamine B as a standard. Figure 2A-C

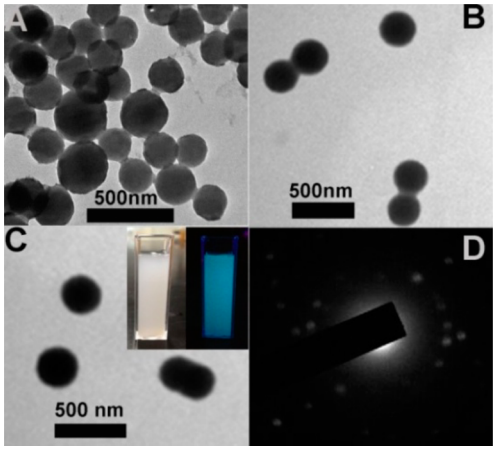

Figure 2. Typical TEM images of the poly(NIPAM-AAm-VPBA)-CDs hybrid microgels with different degree of glucose imprinting for (A) IHM-0, (B) IHM-147, and (C) IHM-295, respectively. The inset in (C) shows the photographs of the aqueous dispersions of the glucose-imprinted poly(NIPAM-AAm-VPBA)-CDs hybrid microgels (IHM-295) under natural light (left) and UV light of 365 nm (right). (D) The SAED pattern of single hybrid microgel particle of IHM-295.

shows the typical TEM images of the resultant poly(NIPAM-AAm-VPBA)-CDs hybrid microgels with different degree of glucose imprinting for IHM-0 (A), IHM-147 (B), and IHM-295 (C), respectively. All the hybrid microgel particles have a spherical shape with an average diameter of about 270, 292, and 309 nm for dried IHM-0, IHM-147, and IHM-295, respectively. Some of the hybrid microgel spheres are connected each other because these TEM samples were prepared from the hybrid microgels dispersed in distilled water exposed in air, which has a pH about 5.8. At this pH, the hybrid microgels are neutral and relatively hydrophobic because the PBA groups are not ionized. When the particles collide together in water, the hydrophobic interactions between the phenyl groups of surface PBA units and the hydrogen bonding interactions between the surface amide groups (from AAm units) or cis-diols (from PBA units) from the neighboring particles can connect the particles together. When the hybrid microgels were dispersed into a 0.005 M PBS buffer of pH 7.4, all the hybrid microgel particles stayed individually (Figure S2A) because small amount of PBA groups will be ionized at this pH and the charge repulsion between these ionized PBA groups push the hybrid microgels away from each other. Based on the particle size distributions of the three hybrid microgels displayed in Figure S2B-D, the calculated standard deviations are ±40, ± 8.9, and ±7.9 nm for IHM-0, IHM-147, and IHM-295, respectively. The TEM images of enlarged single hybrid microgel of IHM-0, IHM-147, and IHM-295 (see Figure S2E-G) clearly demonstrate that the increase in the glucose-imprinting degree increases the radial contrast distribution of the spherical microgel particle. For example, the nonimprinted IHM-0 has nearly uniform density distribution through the whole particle, while the IHM-295 has much darker contrast in the center area than the outer area. This contrast distribution change might be related to the reactivity difference between the relatively hydrophobic free VPBA monomers and the negatively charged glucose-complexed VPBA monomer when copolymerized with the neutral NIPAM and AAm comonomers. In precipitation polymerization, the charged polymer segments prefer to stay on the exterior section of the nuclei particles during the polymerization and microgel growing process. When the aqueous dispersion of the glucose-imprinted poly(NIPAM-AAm-VPBA)-CDs hybrid microgels was exposed to a UV light of 365 nm, blue light was obviously emitted from the hybrid microgel dispersion (inset in Figure 2C for IHM-295). Meanwhile, the HRTEM image of the hybrid microgels (IHM-295) in Figure S3A indicates that the small black CDs are randomly distributed in the polymer microgel matrix. The energy-dispersive X-ray (EDX) spectrum of the hybrid microgels (Figure S3B) shows clear maximum peak positions for C (0.277), O (0.525), and Cu (8.04), but no distinct peaks for B (0.183) and N (0.392) due to their relatively low contents and closeness to the strong C peak. While the Cu is from the copper grid for sample preparation, the C and O should be from both the CDs and poly(NIPAM-AAm-VPBA) microgels. Figure 2D shows a typical SAED pattern of a single IHM-295 hybrid microgel particle. The sharp diffraction spots indicate the presence of single-crystalline nanoparticles in the hybrid microgels. Since the polymers are amorphous, these sharp diffraction spots should come from the fluorescent CDs immobilized in the hybrid microgels, which is confirmed by the similar sharp diffraction spots shown in the SAED pattern of crude CDs (See inset of Figure S1b). The result implies that the CDs have been successfully encapsulated in the glucose-imprinted poly(NIPAM-AAm-VPBA) microgel networks.

To further support the successful embedding of CDs in the hybrid microgels, the glucose-imprinted poly(NIPAM-AAm-VPBA) microgels (using 0.295 g of glucose, noted as IM-295) with no CDs embedded were synthesized for control experiment (see TEM image in Figure S4). Figure 3A shows a comparison of typical UV−visible absorption spectra of the aqueous dispersions of free CDs, glucose-imprinted poly-(NIPAM-AAm-VPBA) microgels (IM-295), and glucose-imprinted poly(NIPAM-AAm-VPBA)-CDs hybrid microgels (IHM-295). There is a clear broad absorption peak centered at 242 nm from the sample of free CDs, which represents the

DOI: 10.1021/acsami.5b04744
ACS Appl. Mater. Interfaces 2015, 7, 15735−15745

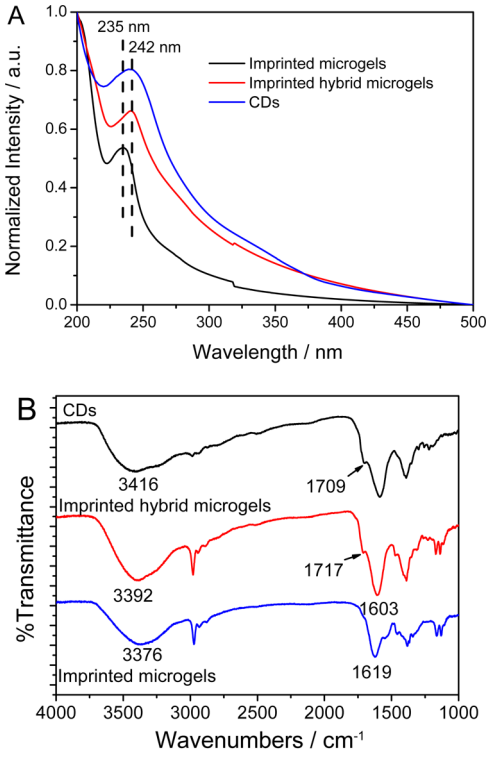

Figure 3. (A) Typical UV−vis absorption spectra and (B) typical FT-IR spectra of the free CDs, glucose-imprinted poly(NIPAM-AAm-VPBA) microgels, and glucose-imprinted poly(NIPAM-AAm-VPBA)-CDs hybrid microgels (IHM-295), respectively.

typical absorption of an aromatic Pi system and is similar to that of polycyclic aromatic hydrocarbons.[41,42] On the other hand, only an absorption peak centered at 235 nm was observed in the glucose-imprinted polymer microgels of IM-295, which should be attributed to the benzene aromatic ring of PBA groups on the polymer chains. In contrast, the glucose-imprinted polymer-CD hybrid microgels of IHM-295 demonstrated a characteristic absorption peak centered at 242 nm from CDs with the absorption at 235 nm from the PBA groups on polymer chains remaining strong, indicating that the CDs have been successfully immobilized into the glucose-imprinted poly(NIPAM-AAm-VPBA) microgels network. It should be mentioned that the weak absorption peak at 235 nm of the microgels has been overshadowed by the strong and broad absorption peak at 242 nm of the CDs immobilized in the hybrid microgels, thus no distinct peak maximum at 235 nm was observed in the hybrid microgels. Nevertheless, the aromatic π systems of the small CDs and the aromatic ring of PBA groups randomly pendant on the microgel network chains should have strong $\pi-\pi$ stacking interactions, which can further help the immobilization of CDs in the interior of the microgels. A comparison of the FT-IR spectra of CDs, IM-295, and IHM-295 can further confirm the stability of the CDs embedded in the microgel networks. As shown in Figure 3B, the free CDs show an apparent broad absorption peak of hydroxyl (−OH) groups at about 3416 cm^{-1} and a characteristic absorption peak at 1709 cm^{-1} of carboxylic acid (−COOH) groups conjugated with condensed aromatic carbons. These hydrophilic −COOH and/or −OH groups on the CDs not only enable the CDs to be dispersed very well in water but also can form hydrogen bonds with the amide groups in the AAm monomers, thus forming CD−AAm complexes in water.[43,44] The formation of the CD-complexed AAm monomer is critical to immobilize the small CDs stably in the interior of the gel network because the AAm monomers can carry the CDs together during the copolymerization and cross-linking process. The broad peak at 3376 cm^{-1} from the IM-295 microgels is attributed to the stretching vibration of the −OH in PBA groups and $-NH_2$ in amide groups on the polymer chains. In the imprinted poly(NIPAM-AAM-VPBA)-CDs hybrid microgels of IHM-295, the surface −OH and/or −COOH groups on CDs have strong hydrogen bonding interactions with the amide $-NH_2$ groups on the polymer chains, thus the stretching vibration energies of these −OH and $-NH_2$ groups change slightly compared to those in free CDs and free IM-295 microgels, resulting in a new maximum IR absorption position centered at 3392 cm^{-1}. The hydrogen bonding interactions between the surface −OH/−COOH groups on CDs and the amide $-NH_2$ on the polymer chains in the IHM-295 hybrid microgels can be further supported by the IR band shift of (1) the C═O stretching of the −COOH groups from 1709 cm^{-1} in free CDs sample to 1717 cm^{-1} in the IHM-295 hybrid microgels and (2) the C═O stretching of the amide ($-CONH_2$) groups from 1619 cm^{-1} in IM-295 polymer microgels to 1603 cm^{-1} in the IHM-295 hybrid microgels. Such strong hydrogen bonding interactions of the surface −OH and/or −COOH groups on CDs with the amide $-NH_2$ groups on the polymer chains enable a very stable immobilization of the small CDs in the interior of the microgel networks. These results also indicate that our one-pot precipitation copolymerization strategy of glucose-complexed VPBA monomers, NIPAM monomers, and CD-complexed AAm monomers is feasible to immobilize the small-sized CDs into the glucose-imprinted poly(NIPAM-AAm-VPBA) microgel network.

3.2. Glucose Sensing Ability of the Hybrid Microgels.

The resultant glucose-imprinted poly(NIPAM-AAm-VPBA)-CDs hybrid microgels demonstrate highly sensitive volume phase transition in response to the increase in glucose concentration at physiological pH. Figure 4A shows the glucose-induced swelling curve of the poly(NIPAM-AAm-VPBA)-CDs hybrid microgels with different glucose-imprinting degrees, in terms of the hydrodynamic radius (R_h) values of the hybrid microgels as a function of glucose concentration, measured in a 5.0 mM PBS of pH 7.40 at 22.0 °C. Without addition of glucose, the R_h of the hybrid microgels of IHM-0, IHM-147, and IHM-295 are 188, 202, and 222 nm, respectively. Clearly, all three hybrid microgels swell with the increase in glucose concentration, because the binding of glucose molecules with the PBA groups on the network chains produces negatively charged boronates and builds up a Donnan potential for the hybrid microgels to swell.[45] Two effects should be noted from the glucose-imprinting on the hybrid microgels. First, the higher the glucose-imprinting degree on the microgel networks, the larger the size of the hybrid microgels synthesized under the same conditions. This result might be attributed to the larger size of the negatively charged glucose-complexed VPBA monomers than the relatively hydrophobic free VPBA monomers. The space originally occupied by the imprinting glucose molecules in the microgel networks enlarges the total size of the hybrid microgels. Second, the higher the glucose-imprinting degree on the microgel networks, the higher the maximum swelling ratio of the hybrid microgels, which indicates a higher glucose sensitivity correspondingly. This result is understandable because the glucose-imprinted boron centers of the PBA groups will serve as favorable glucose

DOI: 10.1021/acsami.5b04744
ACS Appl. Mater. Interfaces 2015, 7, 15735−15745

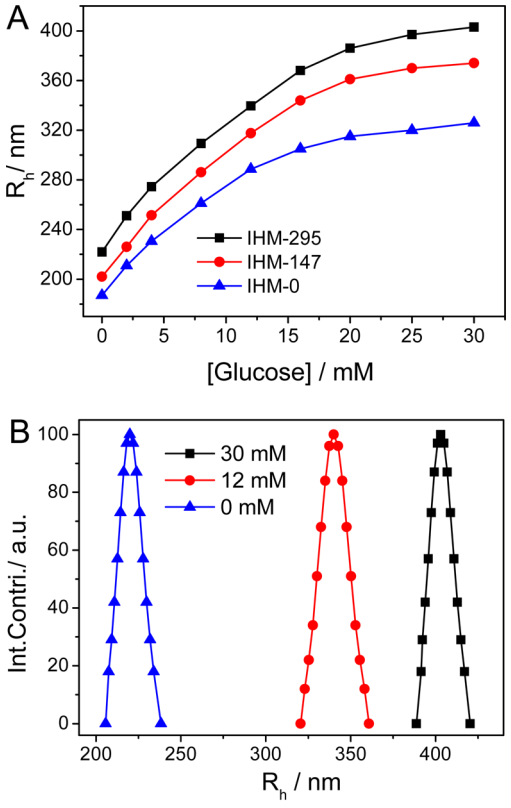

Figure 4. (A) Glucose dependence of the average R_h values of the imprinted poly(NIPAM-AAm-VPBA)-CDs hybrid microgels with different glucose imprinting degree, measured in PBS of pH 7.40 and T = 22 °C. (B) Size distributions of the IHM-295 hybrid microgels measured at different glucose concentrations.

recognition sites to bind more glucose molecules, thus forming more negative charges of the boronate complexes, which induce the gel to swell more. It should be mentioned that all the hybrid microgels are nearly monodispersed regardless of their swelling/shrinking states. As shown in Figure 4B, the imprinted hybrid microgels of IHM-295 demonstrated a very narrow size distribution as glucose concentration gradually increases from 0 to 30 mM. Since the kinetics of the swelling/shrinking transitions of gels depends on the size of the gel particles, the uniform size distribution of the hybrid microgel particles can prevent a signal delay when used for glucose detection. The glucose-sensitive volume phase transition of such nearly monodispersed imprinted hybrid microgels can be also used as a drug carrier for glucose-regulated insulin delivery.

Considering the strong interactions between the surface −OH/−COOH groups on the CDs and the amide groups on the poly(NIPAM-AAm-VPBA) chains, we expect that the glucose-induced swelling of the polymer network chains should change the surface states of the embedded CDs and thus affect the optical properties of the hybrid microgels. To investigate the optical properties of the hybrid microgels, we first compared the photoluminescence (PL) excitation spectra of free CDs, imprinted polymer microgels of IM-295, and imprinted hybrid microgels of IHM-295 (see Figure S5). A comparison of these PL excitation spectra reveals that the excitation peak at 360 nm of the IHM-295 hybrid microgels is associated with the embedded CDs. Figure S6A shows the typical PL spectra of CDs, imprinted microgels of IM-295, and imprinted hybrid microgels of IHM-295 obtained under an excitation wavelength of 360 nm. Both the free CDs and the imprinted poly(NIPAM-AAm-VPBA)-CDs hybrid microgels demonstrated an emission peak at 460 nm, while the imprinted poly(NIPAM-AAm-VPBA) microgels of IM-295 did not, which further proves that the fluorescent CDs have been successfully immobilized in the IHM-295 hybrid microgels. Figure S6B compares the CLSM images of the free CDs, imprinted microgels of IM-295, and imprinted hybrid microgels of IHM-295, obtained from three different excitation wavelengths of 405, 488, and 546 nm, respectively. While the free CDs demonstrated bright fluorescence on the images, the IM-295 microgels containing no CDs did not exhibit detectable fluorescence on the images. In contrast, the IHM-295 hybrid microgels displayed obvious fluorescence on the images, which again confirms the successful immobilization of CDs in the IHM-295 hybrid microgels. The imprinted poly(NIPAM-AAm-VPBA)-CDs hybrid microgels of IHM-295 demonstrate an excellent thermal stability. As shown in Figure S7A, the PL intensity of the imprinted hybrid microgels of IHM-295 remains unchanged within the experimental error after a continuous heating equilibrium at 70 °C for 6 days, which indicates that the newly developed IHM-295 hybrid microgels are very stable and no CDs were released even at a temperature of 70 °C. As shown in the TEM image in Figure S7B, the hybrid microgels remained a spherical morphology after the stability test. Furthermore, Figure S7C shows that the typical UV−vis absorption spectra of the IHM-295 hybrid microgels before and after the stability test are consistent. These results further confirm that our hybrid microgels are very stable. The average PL lifetimes of the free CDs and the imprinted hybrid microgels of IHM-295 are 9.27 and 71.96 ns, respectively, obtained from the time-resolved PL decay profiles (Figure S7D-E). While the average PL lifetime of our CDs carrying surface −COOH/−OH groups is comparable to those CDs with similar surface functional groups,[46] the CDs immobilized in the imprinted hybrid microgels of IHM-295 exhibit a much longer PL lifetime, which could be attributed to the effective protection of the excited state energy from rotational or vibrational loss by rigidifying the surface functional groups conjugated with the aromatic sp^2 carbon system of CDs via the hydrogen bonding interactions with the polymer network chains.[47] Figure 5A shows the evolution of the PL spectra of the glucose-imprinted hybrid microgels of IHM-295 in response to an increase in glucose concentration over a clinically relevant range of 0−30 mM at physiological pH. The hybrid microgels demonstrate glucose-responsive PL spectra with the PL intensity gradually decreased upon the increase in glucose concentration. Compared to the glucose-responsive PL intensity change of the nonimprinted hybrid microgels of IHM-0 (see Figure S8A), it is very clear that the imprinted hybrid microgels of IHM-295 demonstrate a much larger PL intensity change over the same glucose concentration change. For example, the PL intensity of nonimprinted IHM-0 only decreases by 32.1%, but the PL intensity of the imprinted IHM-295 hybrid microgels decreases by 58.4% over the same glucose concentration change from 0 to 30 mM. It should be mentioned that, although we used the PL spectra excited at a wavelength of 360 nm for the glucose sensing study in this work, the CDs in the hybrid microgel sensors can emit strong fluorescence under the excitations of a very broad wavelength range from UV to NIR light (Figure S1e and Figure S8B). The upconverted emissions excited by NIR light provide the hybrid microgels with a big advantage for glucose sensing in biological

DOI: 10.1021/acsami.5b04744
ACS Appl. Mater. Interfaces 2015, 7, 15735−15745

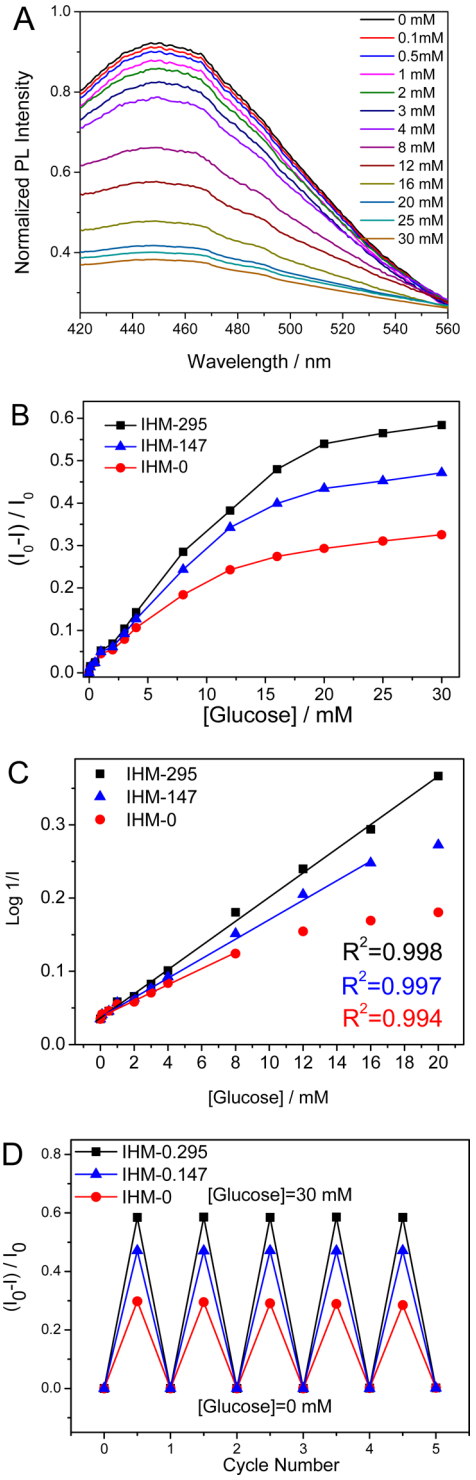

Figure 5. (A) Evolution of PL spectra of the glucose-imprinted IHM-295 hybrid microgels with the increase in glucose concentration from 0 to 30 mM in the PBS of pH 7.40. (B) The quenched PL intensity of the hybrid microgels with different glucose-imprinting degrees as a function of glucose concentration. (C) The linear fitting plots of the glucose dependent PL quenching in terms of $\log(1/I)$ versus glucose concentrations. (D) Reversible PL decay and recovery cycles upon the repeated addition (30.0 mM) and dialysis removal of glucose (0 mM) in the dispersion medium of hybrid microgels.

samples because NIR light has a low energy absorption, maximum penetration, and minimum side effects for human tissue and organs.

To quantitatively correlate the PL signal to the glucose concentration, the decay of PL intensity $(I_0 - I)/I_0$ was plotted against the glucose concentrations, where I_0 and I represent the PL intensity at 460 nm of the hybrid microgels in PBS of pH 7.40 in the absence and presence of different amount of glucose, respectively. As shown in Figure 5B, such plots of the glucose-dependent PL intensity provide clear evidence that the poly(NIPAM-AAm-VPBA)-CDs hybrid microgels can be used for optical glucose detection. A few results can be summarized from the plots. First, the curves of glucose-responsive PL intensity change of the hybrid microgels demonstrated exactly the same trend as the glucose-induced swelling curves shown in Figure 4A, where the hybrid microgels gradually swell with increasing the glucose concentration until stretching to nearly a maximum at higher glucose concentrations. This result implies that the PL quench of the CDs immobilized in the hybrid microgels is induced by the swelling of the microgel networks. Two factors should be considered when the microgels swell up. One is the variation of the Rayleigh scattering due to the decrease in local refractive index of the surrounding medium of the CDs when the gel networks swell.[48,49] Another is the change of surface defects of the CDs. It is known that the nonradiative energy loss paths are highly dependent on the environmental nature surrounding the CDs.[50] When the polymer gel networks swell at higher glucose concentrations, the hydrogen bonding interactions between the polymer chains and the surface −OH/−COOH groups on the CDs will hinder the expansion of hybrid microgels, creating an elastic tension in the bonds at the polymer/CDs interface, thus producing surface states that could quench the PL. Second, the curves in Figure 5B indicate that the glucose-imprinting on the PBA binding sites of the hybrid microgels significantly improves the sensitivity for glucose detection. The higher the glucose-imprinting degree of the hybrid microgels, the larger the quenched PL intensity of the CDs embedded in the microgels corresponding to the same glucose concentration change. Furthermore, the glucose-imprinted hybrid microgels exhibit a broader linear range for glucose detection than the non-imprinted hybrid microgels does. As shown in Figure 5C with a linear fitting of glucose dependent Log(1/I), the linear detection ranges are 0.1−8.0 mM for nonimprinted IHM-0, 0.1−16 mM for partially imprinted IHM-147, and 0.1−20 mM for highly imprinted IHM-295, respectively. While all these three hybrid microgels have a lower detection limit of 0.1 mM, the highly imprinted IHM-295 hybrid microgels have a much higher upper detection linear range (20 mM) than the nonimprinted IHM-0 hybrid microgels that can only reach to 8 mM. Obviously, the improved sensitivity and linear range for glucose detection of the hybrid microgels is associated with the glucose molecular imprinting on the PBA binding sites, which can recognize and bind the glucose molecules with a higher affinity. Figure 5D shows the reversible PL decay and recovery cycles upon the repeated addition (30.0 mM) and dialysis removal of glucose (0 mM) in the dispersion medium of the hybrid microgels. The glucose-PBA binding is reversible. The added glucose molecules complex with the PBA moieties on the gel network chains, forming negatively charged boronate complex that can induce a swelling of gel and thus a quench of PL intensity from CDs. When the glucose molecules were removed from the bathing medium of hybrid microgels, the dissociation equilibrium shifts back from negatively charged boronate ester to noncharged boronic acid, leading to a recovery of both the spectral profiles and intensity. The results

DOI: 10.1021/acsami.5b04744
ACS Appl. Mater. Interfaces 2015, 7, 15735−15745

show that the PL intensity can be recovered by 95.6% and 99.2% of the original basal values for the nonimprinted (IHM-0) and imprinted (IHM-295) hybrid microgels, respectively, after five repeated cycles of glucose addition/removal lasting over 3 weeks. This initial slight decrease in the PL intensity from the repeated glucose addition/removal process could be due to the loss of some CDs bound on the surface of microgels during the repeated dialysis against frequently changed water to remove the glucose. The additional continuous 3 weeks of dialysis of the imprinted hybrid microgels IHM-295 did not show significant fluorescent signal change within the instrumental error. We expect that the dried hybrid microgels can be stored for many years, and the aqueous dispersion of the hybrid microgels can be very stable as long as the solvent is pure. Clearly, the glucose molecular imprinting on the PBA sites of the microgels can further improve the optical signal stability of the hybrid microgels. The excellent signal reproducibility of the glucose-imprinted hybrid microgels indicates that the CDs embedded in the gel networks are highly stable. Such glucose-imprinted poly(NIPAM-AAm-VPBA)-CDs hybrid microgels with highly stable and reproducible fluorescent signals demonstrate a great promise for a new generation of glucose sensors that can continuously and quantitatively monitor the glucose level in solutions.

3.3. Interferences of L-Lactate and Human Serum Albumin on the Glucose Sensing of Hybrid Microgels. As a boronic acid–based glucose sensor, the interference from other cis-diol compounds is a big concern. In general, the concentration of other monosaccharides in blood is very low (<0.1 mM). The major concerned interferents for the boronic acid–based glucose sensors are lactate. Herein, we compared the interferences from lactate on the glucose sensing ability of the nonimprinted and imprinted poly(NIPAM-AAm-VPBA)-CD hybrid microgels, respectively. Figure 6A shows the impact of lactate in a range of concentrations (0, 1, and 5 mM) on the glucose-responsive PL quenching property of the nonimprinted (IHM-0) and imprinted (IHM-295) hybrid microgels. The competitive binding of lactate to the PBA groups in the nonimprinted hybrid microgels reduces the glucose binding degree and, thus, decreases the glucose sensitivity of the nonimprinted hybrid microgel sensor. The more the lactate presented in the detection medium, the larger the deviation of the optical signal reading. The presence of 5 mM lactate caused about 30–40% negative deviation of the glucose-induced PL quenching in the studied glucose concentration range of 2–30 mM. In contrast, the presence of lactate (1 and 5 mM) has negligible effect on the PL quenching in the highly glucose-imprinted IHM-295 hybrid microgel sensor in the whole studied glucose concentration range of 2–30 mM. The result indicates that the glucose-imprinted PBA binding sites can recognize the glucose molecular contour and selectively bind glucose molecules over the lactate molecules. Thus, the IHM-295 hybrid microgels with high population of the imprinted glucose-binding sites of PBA moieties are nearly free of the interferences from lactate. Another concerned interferent is the human serum albumin (HSA). HSA, the most abundant protein in human serum, is known to undergo a slow nonenzymatic glycation process.[6,51] The boronic acid moieties are capable of binding HSA. The addition of glucose and subsequent glycosylation of the HSA protein can further elevate its role as a competitive binder. The initial binding of large HSA molecules to the PBA sites in the microgels can hinder the accessibility of the PBA sites normally accessible to the small

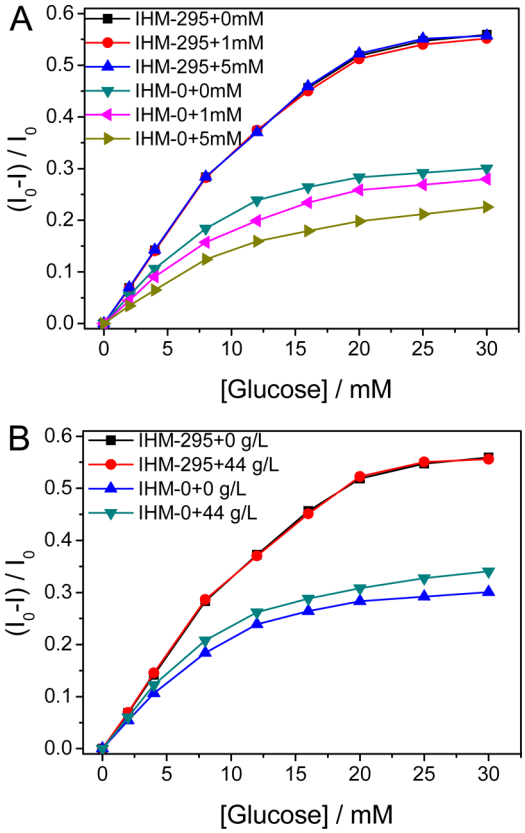

Figure 6. Glucose responsive PL quenching property of the nonimprinted (IHM-0) and imprinted (IHM-295) poly(NIPAM-AAm-VPBA)-CDs hybrid microgels dispersed in PBS buffer of pH 7.40 in the presence of different amounts of (A) L-lactate (0, 1.0, and 5.0 mM) and (B) HSA (0 and 44 g/L), respectively.

glucose molecules. Compared to small glucose molecules, the binding of larger HSA to the PBA sites of microgels causes a larger swelling degree, resulting in a larger degree of PL quenching.[6,13] Figure 6B shows the glucose induced PL quenching of the nonimprinted and imprinted hybrid microgels in the presence of HSA at a concentration of 44 g/L typically found in serum. The result shows that the presence of 44 g/L HSA does increase the glucose-induced PL quenching degree in the nonimprinted hybrid microgel sensor, resulting in about 10–15% positive deviation of the glucose-induced PL quenching in the studied glucose concentration range of 2–30 mM. In contrast, the presence of 44 g/L HSA did not cause significant deviation (<1%) on the glucose sensing ability of the highly imprinted IHM-295 hybrid microgels in the same range of glucose concentration. These results prove that the glucose molecular imprinting on the PBA binding sites of the microgels is successful to reduce the interference from potential major interferents, benefited from the synergistic effects of the glucose molecular contour and the geometrical constraint of the binding sites dictated by the imprinting process. To further test the sensing performance of our imprinted hybrid microgels in real sample, the glucose-induced PL quench curve of the IHM-295 hybrid microgels dispersed in the fetal bovine serum was determined (Figure S9). The results show that the IHM-295 hybrid microgels can sense the glucose concentration in fetal bovine serum as accurately as in PBS buffer when the glucose concentrations was below 12 mM. In the glucose concentration range of 12–30 mM, about 1.0–5.6% deviation of the glucose-

DOI: 10.1021/acsami.5b04744
ACS Appl. Mater. Interfaces 2015, 7, 15735–15745

induced PL quenching in serum was observed when compared to in the PBS buffer. These results prove that our imprinted hybrid microgels have great potential to sense glucose concentration in real biological samples such as serum, tear fluid, and interstitial fluid. The interference of the autofluorescence from these biological samples on our hybrid microgel sensors should be minimal. First, the fluorescent signals from our hybrid microgels immobilized with adequate amount of highly fluorescent CDs are much stronger than the autofluorescence from these biological samples, thus the senor will provide a high signal-to-noise ratio. Second, the fluorescent CDs embedded in the hybrid microgels can emit strong fluorescence in a broad range of wavelength when different excitation wavelengths are used (Figure S1e). The excitation wavelength-tunable fluorescence of the hybrid microgels allows us to select specific emission peak positions for quantitative analysis to avoid the signal overlap with the autofluorescence from the biological sample involved. Third, the hybrid microgels with the CDs immobilized in imprinted polymer networks exhibit a much longer luminescent lifetime (71.96 ns) compared to that of free CDs (9.27 ns), which is favorable for biological use because a fluorescent material with a short luminescence lifetime may suffer interferences from some biological molecules that always have short fluorescent lifetimes.[52] It should be noted that all the glucose-induced PL quench curves in Figure 6 are nonlinear. As we discussed for Figure 5B, the glucose-induced PL quench of the CDs immobilized in the hybrid microgels is induced by the glucose-induced gradual swelling of the cross-linked microgel networks (see Figure 4A). The higher the glucose concentration, the higher the swelling degree of the microgels. However, the swelling degree of the microgels is restricted by the chemical cross-linking of the polymer chains, which will eventually reach to a maximum value.

3.4. In Vitro Toxicity of the Hybrid Microgels. For future glucose sensing in biological applications, the hybrid microgels should be non- or low-cytotoxic. While the highly imprinted poly(NIPAM-AAm-VPBA)-CDs hybrid microgels have demonstrated a great promise for continuous glucose detection with high reproducibility, selectivity, and sensitivity, the safety of the hybrid microgel materials following intentional and unintentional human exposures is definitely a concern. Figure 7 shows the viability of B16F10 cells upon treatment with free CDs, the nonimprinted IHM-0 hybrid microgels, and the highly imprinted IHM-295 hybrid microgels at different concentrations. The results indicated that the cell viability was largely unaffected by the presence of these CDs and poly(NIPAM-AAm-VPBA)-CDs hybrid microgels at concentrations from 25 to 100 μg/mL, which is consistent with the previously reported good biocompatibility of the carbon-based hybrid nanogels in bioapplications.[40] The non- or low cytotoxicity of these hybrid microgels provide a potential for in vivo biological applications.

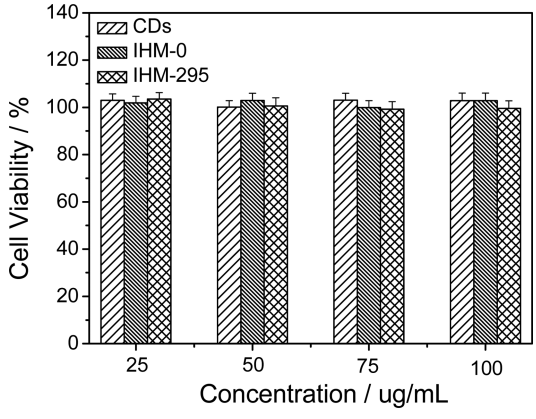

Figure 7. In vitro cytotoxicity of free CDs, nonimprinted (IHM-0) and glucose-imprinted (IHM-295) poly(NIPAM-AAm-VPBA)-CDs hybrid microgels at different concentration.

4. CONCLUSIONS

We have developed a new type of molecularly imprinted hybrid microgels for highly sensitive, highly selective, and continuous glucose detection at physiological pH, based on the immobilization of nontoxic and fluorescent CDs in the molecularly imprinted glucose-sensitive polymer microgels using one-pot free radical precipitation polymerization method. The resultant glucose-imprinted hybrid microgels can reversibly quench and recover the fluorescence signals of the embedded CDs in response to the variation of surrounding glucose concentration, with excellent signal reproducibility resulting from the highly stable immobilization of CDs in the gel networks. The synergistic effects of the glucose molecular contour and the geometrical constraint of the binding sites dictated by the glucose imprinting process can provide the hybrid microgels with high sensitivity and selectivity for glucose detection over a clinically relevant range of 0−30 mM at physiological pH, displaying nearly free of the interference from the potential major interferents of lactate and human serum albumin. In addition, the hybrid microgels exhibit no cytotoxicity in the concentration range of 25−100 μg/mL. The excellent photostability and general robustness of the glucose-imprinted poly(NIPAM-AAm-VPBA)-CDs hybrid microgels make this sensing system ideal for continuous and reliable glucose monitoring under physiological conditions.

■ ASSOCIATED CONTENT

Supporting Information

TEM images, excitation spectra, XPS spectrum, size distribution, and part of PL spectra of the free CDs, glucose-imprinted poly(NIPAM-AAm-VPBA) microgels, and glucose-imprinted poly(NIPAM-AAm-VPBA)-CDs hybrid microgels (Figures S1−S7). The Supporting Information is available free of charge on the ACS Publications website at DOI: 10.1021/acsami.5b04744.

■ AUTHOR INFORMATION

Corresponding Author

* E-mail: shuiqin.zhou@csi.cuny.edu. Tel.: +1 718 982 3897. Fax: +1 718 982 3910.

Notes

The authors declare no competing financial interest.

■ ACKNOWLEDGMENTS

We gratefully acknowledge the financial support from American Diabetes Association (Basic Science Award 1-12-BS-243). We also thank Dr. Probal Banerjee for his kind permission to use his cell culture facility to study the cytotoxicity of our sensor materials.

DOI: 10.1021/acsami.5b04744
ACS Appl. Mater. Interfaces 2015, 7, 15735−15745

REFERENCES

(1) American Diabetes Association. *Diabetes Care*. **2014**, *37*, Supplement 1, S14−S80.10.2337/dc14-S014

(2) Koschwanez, H. E.; Reichert, W. M. In Vitro, In Vivo and Post Explanation Testing of Glucose-Detecting Biosensors: Current Methods and Recommendations. *Biomaterials* **2007**, *28*, 3687−3703.

(3) Durner, J. Clinical Chemistry: Challenges for Analytical Chemistry and The Nanosciences from Medicine. *Angew. Chem., Int. Ed.* **2010**, *49*, 1026−1051.

(4) Steiner, M. S.; Duerkop, A.; Wolfbeis, O. S. Optical Methods for Sensing Glucose. *Chem. Soc. Rev.* **2011**, *40*, 4805−4839.

(5) Nichols, S. P.; Koh, A.; Storm, W. L.; Shin, J. H.; Schoenfisch, M. H. Biocompatible Materials for Continuous Glucose Monitoring Devices. *Chem. Rev.* **2013**, *113*, 2528−2549.

(6) Ward Muscatello, M. M.; Stunja, L. E.; Asher, S. A. Polymerized Crystalline Colloidal Array Sensing of High Glucose Concentrations. *Anal. Chem.* **2009**, *81*, 4978−4986.

(7) Liu, Y.; Zhang, Y. J.; Guan, Y. New Polymerized Crystalline Colloidal Array for Glucose Sensing. *Chem. Commun.* **2009**, 1867−1869.

(8) Yang, X.; Pan, X.; Blyth, J.; Lowe, C. R. Towards The Real-time Monitoring of Glucose in Tear Fluid: Holographic Glucose Sensors with Reduced Interference from Lactate and pH. *Biosens. Bioelectron.* **2008**, *23*, 899−905.

(9) Liu, Y.; Deng, C.; Tang, L.; Qin, A.; Hu, R.; Sun, J. Z.; Tang, B. Z. Specific Detection of D-glucose by A Tetraphenylethene-Based Fluorescent Sensor. *J. Am. Chem. Soc.* **2011**, *133*, 660−663.

(10) Huang, Y. J.; Ouyang, W. J.; Wu, X.; Li, Z.; Fossey, J. S.; James, T. D.; Jiang, Y. B. Glucose Sensing via Aggregation and The Use of "Knock-Out" Binding to Improve Selectivity. *J. Am. Chem. Soc.* **2013**, *135*, 1700−1703.

(11) Wu, W.; Zhou, T.; Berliner, A.; Banerjee, P.; Zhou, S. Glucose-Mediated Assembly of Phenylboronic Acid Modified CdTe/ZnTe/ZnS Quantum Dots for Intracellular Glucose Probing. *Angew. Chem., Int. Ed.* **2010**, *49*, 6554−6558.

(12) Wu, W.; Zhou, T.; Shen, J.; Zhou, S. Optical Detection of Glucose by CdS Quantum Dots Immobilized in Smart Microgels. *Chem. Commun.* **2009**, 4390−4392.

(13) Wu, W.; Zhou, T.; Aiello, M.; Zhou, S. Construction of Optical Glucose Nanobiosensor with High Sensitivity and Selectivity at Physiological pH on The Basis of Organic−Inorganic Hybrid Microgels. *Biosens. Bioelectron.* **2010**, *25*, 2603−2610.

(14) Wu, W.; Shen, J.; Li, Y.; Zhu, H.; Banerjee, P.; Zhou, S. Specific Glucose-to-SPR Signal Transduction at Physiological pH by Molecularly Imprinted Responsive Hybrid Microgels. *Biomaterials* **2012**, *33*, 7115−7125.

(15) Li, Y.; Zhou, S. Facile One-Pot Synthesis of Organic Dye-Complexed Microgels for Optical Detection of Glucose at Physiological pH. *Chem. Commun.* **2013**, *49*, 5553−5555.

(16) Wu, W.; Mitra, N.; Yan, E. C. Y.; Zhou, S. Multifunctional Hybrid Microgel for Integration of Optical Glucose Sensing and Self-Regulated Insulin Release at Physiological pH. *ACS Nano* **2010**, *4*, 4831−4839.

(17) Wu, W.; Chen, S.; Hu, Y.; Zhou, S. A Fluorescent Responsive Hybrid Nanogel for Closed Loop Control of Glucose. *J. Diabetes Sci. Technol.* **2012**, *6*, 892−901.

(18) Wang, D.; Liu, T.; Yin, J.; Liu, S. Stimuli-Responsive Fluorescent Poly(*N*-isopropylacrylamide) Microgels Labeled with Phenylboronic Acid Moieties as Multifunctional Ratiometric Probes for Glucose and Temperatures. *Macromolecules* **2011**, *44*, 2282−2290.

(19) Fan, J.; Jiang, X.; Hu, Y.; Si, Y.; Ding, L.; Wu, W. A Fluorescent Double-Network-Structured Hybrid Microgel as Embeddable Nano-glucometer for Intracellular Glucometry. *Biomater. Sci.* **2013**, *1*, 421−433.

(20) Ye, T.; Jiang, X.; Xu, W.; Zhou, M.; Hu, Y.; Wu, W. Tailoring The Glucose-Responsive Volume Phase Transition Behaviour of Ag@Poly(PhenylboronicAcid)s Hybrid Microgels: from Monotonous Swelling to Monotonous Shrinking upon Adding Glucose at A Physiological pH. *Polym. Chem.* **2014**, *5*, 2352−2362.

(21) Liu, S.; Tian, J.; Wang, L.; Luo, Y.; Sun, X. A General Strategy for The Production of Photoluminescent Carbon Nitride Dots from Organic Amines and Their Application as Novel Peroxidase-Like Catalysts for Colorimetric Detection of H_2O_2 and Glucose. *RSC Adv.* **2012**, *2*, 411−413.

(22) Tian, J.; Liu, S.; Luo, Y.; Sun, X. Fe(III)-Based Coordination Polymer Nanoparticles: Peroxidase-Like Catalytic Activity and Their Application to Hydrogen Peroxide and Glucose Detection. *Catal. Sci. Technol.* **2012**, *2*, 432−436.

(23) Liu, S.; Tian, J.; Wang, L.; Zhang, Y.; Luo, Y.; Li, H.; Asiri, A. M.; Al-Youbi, A. O.; Sun, X. Fast and Sensitive Colorimetric Detection of H_2O_2 and Glucose: A Strategy Based on Polyoxometalate Clusters. *ChemPlusChem* **2012**, *77*, 541−544.

(24) Zhang, Y.; Tian, J.; Liu, S.; Wang, L.; Qin, X.; Lu, W.; Chang, G.; Luo, Y.; Asiri, A. M.; Al-Youbi, A. O.; Sun, X. Novel Application of CoFe Layered Double Hydroxide Nanoplates for Colorimetric Detection of H_2O_2 and Glucose. *Analyst* **2012**, *137*, 1325−1328.

(25) Xing, Z.; Tian, J.; Asiri, A. M.; Qusti, A. H.; Al-Youbi, A. O.; Sun, X. Two-Dimensional Hybrid MesoporousFe_2O_3-Graphene Nanostructures:A Highly Activeand Reusable Peroxidase Mimetic Toward Rapid, Highly Sensitive Optical Detectionof Glucose. *Biosens. Bioelectron.* **2014**, *52*, 452−457.

(26) Tian, J.; Liu, Q.; Asiri, A. M.; Qusti, A. H.; Al-Youbi, A. O.; Sun, X. Ultrathin Graphitic Carbon Nitride Nanosheets: A Novel Peroxidase Mimetic, Fe Doping-mediated Catalytic Performance Enhancement and Application to Rapid, Highly Sensitive Optical Detection of Glucose. *Nanoscale* **2013**, *5*, 11604−11609.

(27) Sun, Y. P.; Zhou, B.; Lin, Y.; Wang, W.; Fernando, K. A. S.; Pathak, P.; Meziani, M. J.; Harruff, B. A.; Wang, X.; Wang, H.; Luo, P. G.; Yang, H.; Kose, M. E.; Chen, B.; Veca, L. M.; Xie, S. Y. Quantum-Sized Carbon Dots for Bright and Colorful Photoluminescence. *J. Am. Chem. Soc.* **2006**, *128*, 7756−7757.

(28) Yang, S.; Wang, X.; Wang, H.; Lu, F.; Luo, P. G.; Cao, L.; Meziani, M. J.; Liu, J.; Liu, Y.; Chen, M.; Huang, Y.; Sun, Y. Carbon Dots as Nontoxic and High-Performance Fluorescence Imaging Agents. *J. Phys. Chem. C* **2009**, *113*, 18110−18114.

(29) Baker, S. N.; Baker, G. A. Luminescent Carbon Nanodots: Emergent Nanolights. *Angew. Chem., Int. Ed.* **2010**, *49*, 6726−6744.

(30) Esteves da Silva, J. C. G.; Gonçalves, H. M. R. Analytical and Bioanalytical Applications of Carbon Dots. *TrAC, Trends Anal. Chem.* **2011**, *30*, 1327−1336.

(31) Luo, P. G.; Yang, F.; Yang, S. T.; Sonkar, S. K.; Yang, L.; Broglie, J. J.; Liu, Y.; Sun, Y. P. Carbon-Based Quantum Dots for Fluorescence Imaging of Cells and Tissues. *RSC Adv.* **2014**, *4*, 10791−10807.

(32) Nie, H.; Li, M.; Li, Q.; Liang, S.; Tan, Y.; Sheng, L.; Shi, W.; Zhang, S. X. Carbon Dots with Continuously Tunable Full-Color Emission and Their Application in Ratiometric pH Sensing. *Chem. Mater.* **2014**, *26*, 3104−3112.

(33) Ding, C.; Zhu, A.; Tian, Y. Functional Surface Engineering of C-Dots for Fluorescent Biosensing and in Vivo Bioimaging. *Acc. Chem. Res.* **2014**, *47*, 20−30.

(34) Zheng, X. T.; Ananthanarayanan, A.; Luo, K. Q.; Chen, P. Glowing Graphene Quantum Dots and Carbon Dots: Properties, Syntheses, and Biological Applications. *Small* **2014**, *10*, 1−17.

(35) Xu, M.; He, G.; Li, Z.; He, F.; Gao, F.; Su, Y.; Zhang, L.; Yang, Z.; Zhang, Y. A Green Heterogeneous Synthesis of N-Doped Carbon Dots and Their Photoluminescence Applications in Solid and Aqueous States. *Nanoscale* **2014**, *6*, 10307−10315.

(36) Yang, Z.; Li, Z.; Xu, M.; Ma, Y.; Zhang, J.; Su, Y.; Gao, F.; Wei, H.; Zhang, L. Controllable Synthesis of Fluorescent Carbon Dots and Their Detection Application as Nanoprobes. *Nano-Micro Lett.* **2013**, *5*, 247−259.

(37) Shen, P.; Xia, Y. Synthesis-Modification Integration: One-Step Fabrication of Boronic Acid Functionalized Carbon Dots for Fluorescent Blood Sugar Sensing. *Anal. Chem.* **2014**, *86*, 5323−5329.

(38) Haupt, K.; Mosbach, K. Molecularly Imprinted Polymers and Their Use in Biomimetic Sensors. *Chem. Rev.* **2000**, *100*, 2495−2504.

(39) Cai, D.; Ren, L.; Zhao, H.; Xu, C.; Zhang, L.; Yu, Y.; Wang, H.; Lan, Y.; Roberts, M. F.; Chuang, J. H.; Naughton, M. J.; Ren, Z.;

DOI: 10.1021/acsami.5b04744
ACS Appl. Mater. Interfaces 2015, 7, 15735−15745

Chiles, T. C. A Molecular-Imprint Nanosensor for Ultrasensitive Detection of Proteins. *Nat. Nanotechnol.* **2010**, *5*, 597−601.
(40) Wang, H.; Ke, F.; Mararenko, A.; Wei, Z.; Banerjee, P.; Zhou, S. Responsive Polymer−Fluorescent Carbon Nanoparticle Hybrid Microgels for Optical Temperature Sensing, Near-Infrared Light Responsive Drug Release, and Tumor Cell Imaging. *Nanoscale* **2014**, *6*, 7443−7452.
(41) Wang, H.; Shen, J.; Li, Y.; Wei, Z.; Cao, G.; Gai, Z.; Hong, K.; Banerjee, P.; Zhou, S. Magnetic Iron Oxide−Fluorescent Carbon Dots Integrated Nanoparticles for Dual-Modal Imaging, Near-Infrared Light-Responsive Drug Carrier and Photothermal Therapy. *Biomater. Sci.* **2014**, *2*, 915−923.
(42) Yu, S. J.; Kang, M. W.; Chang, H. C.; Chen, K. M.; Yu, Y. C. Bright Fluorescent Nanodiamonds: No Photobleaching and Low Cytotoxicity. *J. Am. Chem. Soc.* **2005**, *127*, 17604−17605.
(43) Zheng, L.; Chi, Y.; Dong, Y.; Lin, J.; Wang, B. Electrochemiluminescence of Water-Soluble Carbon Nanocrystals Released Electrochemically from Graphite. *J. Am. Chem. Soc.* **2009**, *131*, 4564−4565.
(44) Fang, Y.; Guo, S.; Li, D.; Zhu, C.; Ren, W.; Dong, S.; Wang, E. Easy Synthesis and Imaging Applications of Cross-Linked Green Fluorescent Hollow Carbon Nanoparticles. *ACS Nano* **2012**, *6*, 400−409.
(45) Zhang, Y.; Guan, Y.; Zhou, S. Q. Synthesis and Volume Phase Transitions of Glucose-Sensitive Microgels. *Biomacromolecules* **2006**, *7*, 3196−3201.
(46) Guo, Z.; Zhang, Z.; Zhang, W.; Zhou, L.; Li, H.; Wang, H.; Andreazza-Vignolle, C.; Andreazza, P.; Zhao, D.; Wu, Y.; Wang, Q.; Zhang, T.; Jiang, K. Color-Switchable, Emission-Enhanced Fluorescence Realized by Engineering C-dot@C-dot Nanoparticles. *ACS Appl. Mater. Interfaces* **2014**, *6*, 20700−20708.
(47) Wang, Y.; Hu, A. Carbon Quantum Dots: Synthesis, Properties and Applications. *J. Mater. Chem. C* **2014**, *2*, 6921−6939.
(48) Contreras-Caceres, R.; Sanchez-Iglesias, A.; Karg, M.; Pastoriza-Santos, I.; Perez-Juste, J.; Pacifico, J.; Hellweg, T.; Fernández-Barbero, A.; Liz-Marzán, L. M. Encapsulation and Growth of Gold Nanoparticles in Thermoresponsive Microgels. *Adv. Mater.* **2008**, *20*, 1666−1670.
(49) Alvarez-Puebla, R. A.; Contreras-Caceres, R.; Pastoriza-Santos, I.; Perez-Juste, J.; Liz-Marzán, L. Au@pNIPAM Colloids as Molecular Traps for Surface Enhanced, Spectroscopic, Ultra-Sensitive Analysis. *Angew. Chem., Int. Ed.* **2009**, *48*, 138−143.
(50) Wang, X.; Cao, L.; Lu, F.; Meziani, M. J.; Li, H.; Qi, G.; Zhou, B.; Harruff, B. A.; Kermarrec, F.; Sun, Y. P. Photoinduced Electron Transfers with Carbon Dots. *Chem. Commun.* **2009**, 3774−3776.
(51) Burtis, C. A.; Ashwood, E. R. (Eds.) *Tietz Textbook of Clinical Chemistry*, 3rd ed.; W. B. Saunders: Philadelphia, PA, 1999.
(52) Guo, C. X.; Xie, J.; Wang, B.; Zheng, X.; Yang, H.; Li, C. M. A New Class of Fluorescent-Dots: Long Luminescent Lifetime Bio-Dots Self-assembled from DNA at Low Temperatures. . *Sci. Rep.* **2013**, *3*, 2957:1−6.

DOI: 10.1021/acsami.5b04744
ACS Appl. Mater. Interfaces 2015, 7, 15735−15745